

HEARES 01411

## Sensitivity for interaural time and intensity difference of auditory midbrain neurons in the grassfrog

Willem J. Melssen, Willem J.M. Epping \* and Ivo H.M. van Stokkum \*\*

*Department of Medical Physics and Biophysics, University of Nijmegen, The Netherlands*

(Received 11 January 1990; accepted 25 March 1990)

The sensitivity for interaural time (ITD) and intensity (IID) difference was investigated for single units in the auditory midbrain of the grassfrog. A temporally structured stimulus was used which was presented by means of a closed sound system. At best frequency (BF) the majority of units was selective for ITD as indicated by an asymmetrically (73%) or symmetrically (7%) shaped ITD-rate histogram. About 20% appeared to be nonselective. Units with a symmetrical rate histogram had BFs well above 0.9 kHz, whereas for the other categories no relationship with BF was observed. Most units had a selectivity for ITD which was rather independent from frequency and absolute intensity level. In 62% of the units interaural time difference could be traded by interaural intensity difference. In most cases this so-called time-intensity trading could be explained by the intensity-latency characteristics of auditory nerve fibres. About 20% was sensitive to IID only and 5% to ITD only. A binaural model is proposed which is based on the intensity-rate and intensity-latency characteristics of auditory nerve fibres, the linear summation of excitatory and inhibitory post synaptic potentials in second order neurons, and spatiotemporal integration at the level of third order neurons. By variation of only a small number of parameters, namely strengths and time constants of the connectivities, the range of experimentally observed response patterns could be reproduced.

Amplitude modulation; Binaural modelling; Grassfrog; Interaural time- and intensity difference; Sound localization; Torus semicircularis

---

*Correspondence to:* Willem J. Melssen, Department of Medical Physics and Biophysics, University of Nijmegen, P.O. Box 9101, 6525 EZ Nijmegen, The Netherlands.

---

\* *Present address:* Koninklijke Shell Exploration and Production Laboratory, Department of General Research and Mathematics, Volmerlaan 6, NL-2288 GD Rijswijk ZH, The Netherlands.

\*\* *Present address:* Faculty of Physics and Astronomy, Free University, De Boelelaan 1081, NL-1081 NV Amsterdam, The Netherlands.

*Abbreviations:* BF = best frequency; CITD = cut-off interaural time difference; CPI = constant pulse intensity; DMN = dorsal medullary nucleus; IID = interaural intensity difference; IPI = increasing pulse intensity; ITD = interaural time difference; LT = latency; NVIII = auditory nerve; PSP = post synaptic potential; RW = response width; SI = synchronization index; SON = superior olivary nucleus; SPL = sound pressure level; TR = trading ratio; TS = torus semicircularis.

### Introduction

Anurans can not rely on the same mechanisms used for sound localization as higher vertebrates do. Because anurans lack external ears, interaural spectral differences can be excluded as a possible cue for the localization of sound (Eggermont, 1988). The interaural distance of frogs and toads is small compared to the wavelengths anurans use for acoustical communication. Therefore, external interaural intensity differences (IIDs) are 2 dB at maximum (Michelsen et al., 1986). Anurans, however, are able to localize species-specific sounds (e.g. Walkowiak and Brzoska, 1982) with an accuracy of about 15° in the azimuthal plane (Rheinländer et al., 1979; Klump and Gerhardt, 1989). The demonstrated accuracy corresponds to interaural time and intensity differences of about 10 µs and 1 dB respectively (Aertsen et al., 1986,

Fay and Feng, 1987). If the anuran ear would act as a pressure receiver, as is the case in higher vertebrates, it is almost impossible for the central nervous system to detect these minute interaural disparities. Moreover, the relatively low body temperature (15°C) of anurans causes the nervous system to be relatively imprecise.

Anurans, however, are equipped with a specialized acoustic periphery. Both middle ears have an open connection with the mouth cavity via the large eustachian tubes, and possibly also with the lungs (Narins et al., 1988). The displacement of the eardrum is the result of interference of sound coming directly from the outside and sound conducted through internal pathways. Thus, the anuran ear acts more like a pressure-gradient receiver (Feng and Shofner, 1981). By this mechanism the directionality of the acoustic periphery is increased substantially and the interaural difference of eardrum displacement can be as large as 10 dB (Pinder and Palmer, 1983; Vlaming et al., 1984; Michelsen et al., 1986).

Because of the intensity-latency characteristics of auditory nerve (NVIII) fibres, IIDs are transformed into rate and latency differences which can be as large as 15 spikes/dB and 1.4 ms/dB, respectively (Feng and Capranica, 1976, 1978; Feng, 1982). These interaural time differences (ITDs) are quite easily detectable by the central nervous system (Fay and Feng, 1987). On the basis of the NVIII intensity-latency function, one may expect a relation between the selectivities for ITD and IID in neurons receiving binaural input. Moreover, the relation between intensity and latency allows us to study the effects of interaural latency differences upon neural responses independent from the differences in ipsi- and contralateral firing rate.

In most studies sensitivity for ITD and IID has been explored with rather simple stimulus ensembles: unmodulated tones, acoustic clicks and broadband noise (e.g. Feng and Capranica, 1976, 1978; Irvine, 1987; Melssen and Epping, 1990; Yin et al., 1987). In this study stimuli consist of trains of pulses which closely resemble the frog's mating call. Many neurons in the dorsal medullary nucleus (DMN), in the superior olivary nucleus (SON) as well as neurons in the torus semicircularis respond vigorously to such pulse trains

(Walkowiak, 1984; Schneider-Lowitz, 1983). Therefore, the use of temporally structured stimuli is a more natural and powerful way to study mechanisms underlying the sensitivity for IID and ITD.

Experiments were conducted in the torus semicircularis (TS) of the grassfrog (*Rana temporaria* L.), which is regarded as the homologue of the inferior colliculus in higher vertebrates. First, an investigation into the neural response types to ITD stimulation has been performed. The relations between, on the one hand, ITD selectivity and, on the other hand, best frequency (BF), response latency and degree of time-locking were examined. To gain insight into a possible dependency of the observed ITD selectivities on other stimulus parameters, a number of TS units was tested with different carrier frequencies and at various absolute intensity levels. Second, time-intensity trading of auditory midbrain neurons was investigated by a combined ITD-IID stimulus.

A model is proposed which mimicks the different types of selectivity for IID and ITD that are observed in the auditory midbrain of the grassfrog. This model is based on 1) the NVIII intensity-rate and intensity-latency functions (Feng, 1982), 2) the interaction of excitatory and inhibitory post synaptic potentials at the level of the DMN or SON, and 3) spatiotemporal integration in the torus semicircularis.

## Methods

Single unit recordings were made in the torus semicircularis of the immobilized grassfrog. Animal preparation, acoustic stimulus presentation and recording procedure have been described in detail in Melssen and Epping (1990). The stimulus presentation will be described only briefly.

### *Acoustic stimulus presentation*

Stimuli were presented through a closed sound system. In order to separate effects due to interference in the acoustic periphery and effects originating from binaural neural interaction the frog's mouth was kept open during stimulation. The amplitude response of the sound system was flat within 5 dB for frequencies between 0.1 and

3.2 kHz, which is a sufficient range for studying the auditory system of the grassfrog (Brzoska et al., 1977). Phase characteristics were smooth. Differences in amplitude and phase of both couplers were less than 2 dB and  $30^\circ$  (at 0.5 kHz), respectively. Usually, stimuli were presented at intensities in the range of 70–90 dB peak SPL (relative to  $20 \mu\text{N/m}^2$ ). These intensities are sufficient to evoke behavioural responses (Walkowiak and Brzoska, 1982; Brzoska 1984). As a search stimulus a sequence of tonepips, noise bursts, natural and artificial mating call variations was used (Van Stokkum, 1987). For units with very low thresholds, which could experience internal acoustic crosstalk through the acoustic periphery (Feng and Capranica, 1976), stimulus intensities less than 30 dB above threshold were applied.

### Stimulus ensemble

Sensitivity for ITD and IID was investigated with equidistant pulse trains which were presented dichotically. Interaural time and intensity difference were varied systematically. In the first type of stimulation (Fig. 1) the amplitude of the pulses in each train was constant (constant pulse intensity, CPI). In the second type, the amplitude

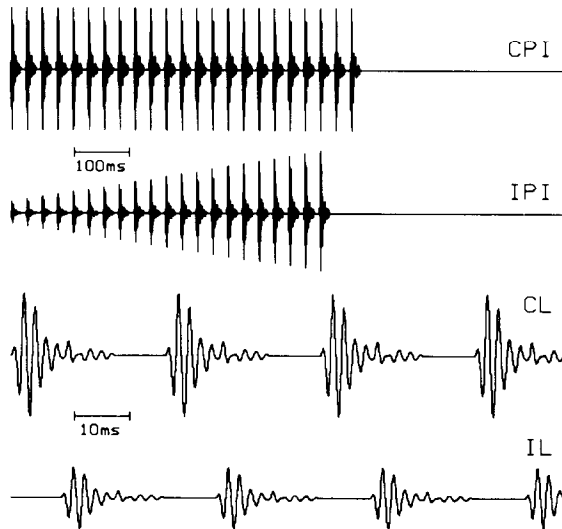


Fig. 1. Constant pulse intensity (CPI) and increasing pulse intensity (IPI) trains. The lower two traces represent a contralateral (CL) and an ipsilateral (IL) CPI pulse train-pair presented at ITD = +9 ms and IID = -6 dB. Carrier frequency is 0.5 kHz. Note the different time scales.

of the pulses was increased linearly (increasing pulse intensity, IPI). Thereby the intensity difference between the first and last pulse of each train was -20 dB. The pulse repetition rate was 35/s. The number of pulses was 23 for the CPI stimulus and 21 for IPI. The pulse envelope (duration 20 ms, on-off ratio 0.75) was taken from an original mating call of the grassfrog. Usually, best frequency was used as carrier frequency. Each train was presented once per three seconds whereby the sound intensity (causing an interaural intensity difference) or the stimulus-onset (causing an interaural time difference) at the ipsilateral ear were varied. To check the reproducibility of responses each stimulus sequence was repeated at least 5 times. In the combined ITD-IID stimulus, IIDs ranged from -12 up to +12 dB in steps of 4 dB and ITD values were -5, -3, -1, 0, 1, 3 and 5 ms, respectively. With positive IIDs the ipsilateral ear is stimulated more intensely than the contralateral ear. A positive ITD indicates a lag of the ipsilateral pulse trains (Fig. 1). To study sensitivity for ITD in finer detail, a similar stimulus was presented at a constant binaural intensity (IID = 0). Here, ITDs were varied pseudorandomly between 0,  $\pm 0.3$ ,  $\pm 0.6$ ,  $\pm 0.9$ ,  $\pm 1.2$ ,  $\pm 1.5$ ,  $\pm 2.0$ ,  $\pm 2.5$ ,  $\pm 3.0$ ,  $\pm 6.0$ , and  $\pm 9.0$  ms. To minimize habituation effects, at the start three pulse trains with ITD = 0 ms were presented which were excluded from the analysis.

### Data analysis

Neural responses were represented by event displays, reordered according to the stimulus parameter(s) of interest. Furthermore, the average firing rate as function of stimulus parameter was represented by means of rate histograms. The event display was considered to be an estimate of a unit's sensitivity for the applied stimulus parameter (Epping and Eggermont, 1985a). In case units exhibited spontaneous activity, a time window was applied to separate stimulus evoked events from spontaneous discharges. The time window was estimated from the peri stimulus time histogram. The response latency (LT) was defined by the time elapsed between the onset of the pulse train at the excitatory (mostly the contralateral) ear and the first occurrence of a stimulus evoked neural event.

The degree of time-locking to the stimulus-envelope was studied by means of the synchronization index (SI) or vector strength (Goldberg and Brown, 1969). For each ITD or ITD-IID combination, the SI was computed from the corresponding period histogram. The cycle-time of the period histogram was 28 ms, which is equal to the time-interval between two consecutive pulses. The significance of time-locking was tested with the Rayleigh test for circular data (Hillery and Narins, 1987; Mardia, 1972).

From the rate histograms, obtained with ITD stimulation, the so-called ITD response width (RW) and cut-off interaural time difference (CITD) were determined. Both RW and CITD serve as measures of the degree of ITD selectivity. The RW was defined as the difference between those ITDs where the rate histogram was at 20% and 80% of maximum, respectively. The CITD was defined by the ITD at which the firing rate was reduced to 50% of the maximum.

The average response rates to the ITD-IID stimulus were arranged into a two-dimensional rate matrix  $F(\Delta T, \Delta I)$ . Each column in this matrix represents the averaged rate as function of IID given a particular ITD whereas each row represents the ITD-rate function given a particular IID. The two-dimensional rate matrix  $F$  was approximated by a second degree polynomial function  $f$ :

$$f(\Delta T, \Delta I) = a_0 + a_1 \Delta T + a_2 \Delta I + a_3 \Delta I \Delta T \\ + a_4 \Delta T^2 + a_5 \Delta I^2 \quad (1)$$

For this purpose a fit-procedure (HFTI algorithm, Lawson and Hanson, 1974) was applied which yielded a (minimum norm) least squares solution, i.e. the parameters  $a_0$ – $a_5$ . These parameters indicated in how far response rate depended in a (non)linear way on interaural time and intensity difference. The quality of the fit was expressed by the mean square error. A small mean square error indicated a nearly perfect fit of the rate function  $f(\Delta T, \Delta I)$ . For fits with a mean square error less than 0.5, we determined the so-called trading ratio coefficient (TR) which serves as a measure of the degree of time-intensity trading. Therefore the ratio of the partial derivatives  $\partial f / \partial \Delta I$  and

$\partial f / \partial \Delta T$  was averaged over both  $\Delta T$  and  $\Delta I$ . For instance, if time is traded by intensity in a linear way, thus if the parameters  $a_3$  up to  $a_5$  are approximately zero, then the trading ratio is equal to  $TR = a_2 / a_1$ . A TR equal to 0.25 ms/dB means that a change of 0.25 ms in ITD can be counteracted by a simultaneous IID change of 1 dB. An infinite TR indicates that a unit is only sensitive for IID, whereas a TR equal to zero corresponds to a sensitivity for ITD only.

### *The binaural model*

Our main goal was to study the mechanisms, which underly the sensitivity for ITD and IID of second (DMN, SON) and third order (TS) neurons. Because of the decoupling of the periphery by the open mouth, there was no need to incorporate properties of the anuran acoustic periphery (Aertsen et al., 1986). It was beyond the scope of the present paper to model explicitly properties of the peripheral auditory pathway, i.e. the amphibian and basilar papillae and the auditory nerve. Instead, the functionality of the peripheral pathway was translated into representative intensity-rate and intensity-latency functions. For this purpose, we first averaged the rate and latency functions of NVIII fibres, as determined by Feng (1982). Feng's original dataset (thin lines) is depicted in Fig. 2 (upper panel). Next, the averaged rate function was estimated by a sigmoidal function  $R(I)$ :

$$R(I) = R_0 \exp[\alpha(I\Theta(I) - m)] \\ / (1 + \exp[\alpha(I\Theta(I) - m)]) \quad (2)$$

The parameters  $R_0$  and  $\alpha$  determine the maximum firing rate and the steepness of the rate function, respectively. The parameter  $m$  determines the onset of the sigmoidal curve and thereby the level of spontaneous activity of the NVIII fibres. The variable  $I$  denotes the sound intensity relative to the fibres threshold. Both  $I$  and  $m$  are expressed in dB. The Heaviside function  $\Theta(I)$  is equal to 1 for  $I > 0$ , otherwise 0. The averaged latency function was fitted by the function  $L(I)$ :

$$L(I) = L_0 + \beta / I; \quad I > 0 \quad (3)$$

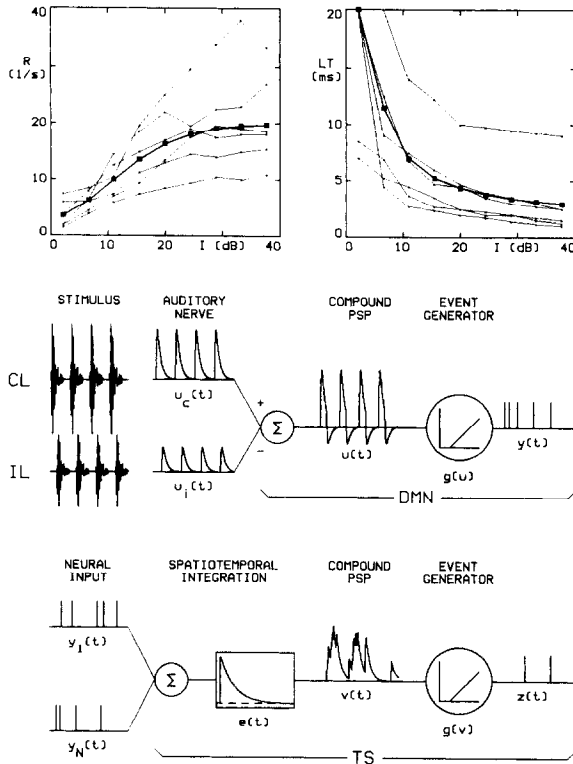


Fig. 2. The binaural model. The thin lines in the upper panel represent rate and latency functions of auditory nerve fibres (Feng, 1982). Filled squares indicate points on the averaged rate and latency functions and fitted rate and latency curves are represented by bold lines. Data were used with kind permission of A.S. Feng. Horizontal axes denote intensity level relative to threshold. Vertical axes represent firing rate ( $R$ ) and response latency ( $LT$ ), respectively. The middle traces illustrate the peripheral part of the model. The model was driven by contralateral (CL) and ipsilateral (IL) pulse trains. The lower trace depicts more central processing stages in a schematical way: event-summation and synaptic low-pass filtering. See text for a more detailed description.

For  $I \leq 0$  the latency function  $L(I)$  was set to infinity. The parameter  $L_0$  represents the asymptotic response latency and  $\beta$  determines the concavity of the latency curve. The fit-functions  $R(I)$  and  $L(I)$  are also shown in Fig. 2 as bold lines. Estimated parameters of the rate and latency functions are provided in Table III (see Results). In the sequel,  $R(I)$  and  $L(I)$  will be referred to as the rate and latency functions. Stimulation of one ear with a single sound pulse results in the activation of a group of NVIII fibres (Fig. 2, middle trace). It was assumed that fibres are tuned

to the same frequency and have the same threshold. Short term adaptation (Megela and Capranica, 1981; Eggermont, 1985; Zelik and Narins, 1985) was not incorporated and therefore, each presented pulse yields the same activation pattern. The evoked activity in the contra- and ipsilateral NVIII is represented by  $u_c(t)$  and  $u_i(t)$  respectively. Apart from a scaling factor,  $u_k(t)$  ( $k = i, c$ ) resembles the peri stimulus time histogram obtained from the activity of a group of NVIII fibres. For a single sound pulse presented to one ear at time  $t = 0$ ,  $u_k(t)$  reads:

$$u_k(t) = w_k R(I) \exp[-(t - L(I))/\tau_{kd}] \times (1 - \exp[-(t - L(I))/\tau_{ku}]);$$

$$k = i, c \quad (4)$$

The parameter  $w_k$  can be regarded as the strength of the synaptic coupling between NVIII fibres and second order neurons. The time constants  $\tau_{kd}$  and  $\tau_{ku}$ , which model the degree of synchronization of NVIII activity as well as integrative properties of DMN units, determine the shape, i.e. the decay ( $\tau_{kd}$ ) and rise ( $\tau_{kd}\tau_{ku}/(\tau_{kd} + \tau_{ku})$ ), of  $u_k(t)$ . The compound post synaptic potential (PSP), also called generatorpotential, is equal to  $u(t) = u_i(t) + u_c(t)$ . Note that for  $w_i = -w_c$  the spontaneous activity levels of both NVIIIs cancel and hence  $u(t) = 0$ . Thusfar, our model shows many similarities with previous models on binaural interaction (e.g. Van Bergeijk, 1962; Itoh, 1984; Kuwada and Yin, 1987). In the next stage, action potentials are generated stochastically with help of a generator function  $g(u)$ , also known as the intensity function in point process literature (Cox and Isham, 1980). The firing probability of a unit in an interval with duration  $\Delta t$  is equal to

$$P[dN(t + \Delta t) = 1 | u(t) = u] = 1 - \exp[-g(u) \Delta t] \quad (5)$$

where  $N(t)$  is the counting process, representing the total number of events up to time  $t$ , and  $dN(t) = N(t + \Delta t) - N(t)$  (Van Stokkum and Gielen, 1989). In all simulations the interval  $\Delta t$

was 0.1 ms. In the present model pulse generation was semilinear:

$$g(u) = (u + a)\Theta(u + a) \quad (6)$$

The parameter  $a$  can be used to model either the spontaneous activity level of a unit ( $a > 0$ ) or a threshold mechanism ( $a < 0$ ). Absolute refractory time ( $\tau_{abs}$ ) was included by means of a period of zero probability following a generated event. The output of neurons can mathematically be described as  $y(t) = \sum_{i=1}^N \delta(t - t_i)$ , where  $\delta(t)$  is the Dirac delta-function and  $t_i$  the time of occurrence of the  $i^{\text{th}}$  event.

In the next stage of the model (Fig. 2, lower part) spatiotemporal integration was included. The convergence of the output of  $N$  second order DMN neurons, i.e.  $y_1(t)$  up to  $y_N(t)$ , to a third order TS neuron is modelled as linear summation of events, followed by low-pass filtering (Rall, 1977). The resulting post synaptic potential  $v(t)$  is expressed by

$$v(t) = \sum_{i=1}^N \int_{-\infty}^t ds e(s) y_i(t - s) \quad (7)$$

where the excitatory post synaptic potential  $e(t)$  can be written as

$$e(t) = e_0 \exp[-t/\tau_d](1 - \exp[-t/\tau_u])\Theta(t) \quad (8)$$

In analogy with Eq. 4,  $\tau_u$  and  $\tau_d$  determine the shape of the excitatory post synaptic potential. Finally, the TS unit had a generator function equal to  $g(v) = (v + b)\Theta(v + b)$ . Again, event series  $z(t)$  were generated according to Eq. 5.

## Results

Experiments were made throughout the year except for the winter season. Single unit activity was recorded in 24 grassfrogs, both males and females. Depending on the stability of the recording, stimuli were presented at several sound intensity levels and carrier frequencies. Spontaneous activity, the presence of which was defined as at least one discharge per 10 s in absence of an

external stimulus, was exhibited by 30 units (25%). More than 80% of these units had spontaneous firing rates less than 2/s. The majority (81%) of TS units responded in a reproducible and stationary way, i.e. responses were constant over time.

### *Sensitivity for interaural time difference*

Sensitivity for ITD was investigated with equidistant pulse trains presented at both ears whereby the interaural time difference was varied. Depending on the response properties of a particular unit, the most effective paradigm, i.e. CPI or IPI, was chosen. The CPI method was applied to units which were not responsive to a single stimulus pulse, they required temporal integration over two or more pulses. The IPI method was applied to units which exhibited strong adaptation to CPI trains. In 215 stimulus presentations the activity of 116 neurons was recorded. Three neurons were totally inhibited during CPI or IPI stimulation and 5 units had responses which were not reproducible. These eight units were not considered for further analyses.

### *Classification of response type*

Neural responses are represented by event displays, ITD-rate and ITD-synchronization index histograms (Fig. 3). Classification of ITD response type was performed on the basis of the shape of the rate histogram. Responses of six representative TS units are depicted in the first column. Responses in the second and third column will be discussed later.

Unit 321-700 (Fig. 3a) responded with one spike to each sound pulse, with strong locking to the stimulus envelope. This is also evident in the ITD-SI histogram (mean SI = 0.98). The mean SI was obtained by averaging over all non-zero bins in the SI histogram. This short latency unit (LT = 19 ms) was not selective for ITD, as indicated by the flat ITD-rate histogram. For monaural stimuli, this unit responded only to contralateral stimulus presentations.

Fig. 3b shows another nonselective unit, which responded less vigorously with approximately 2 spikes only to the whole pulse train. Response latency was 60 ms and no locking to the pulses

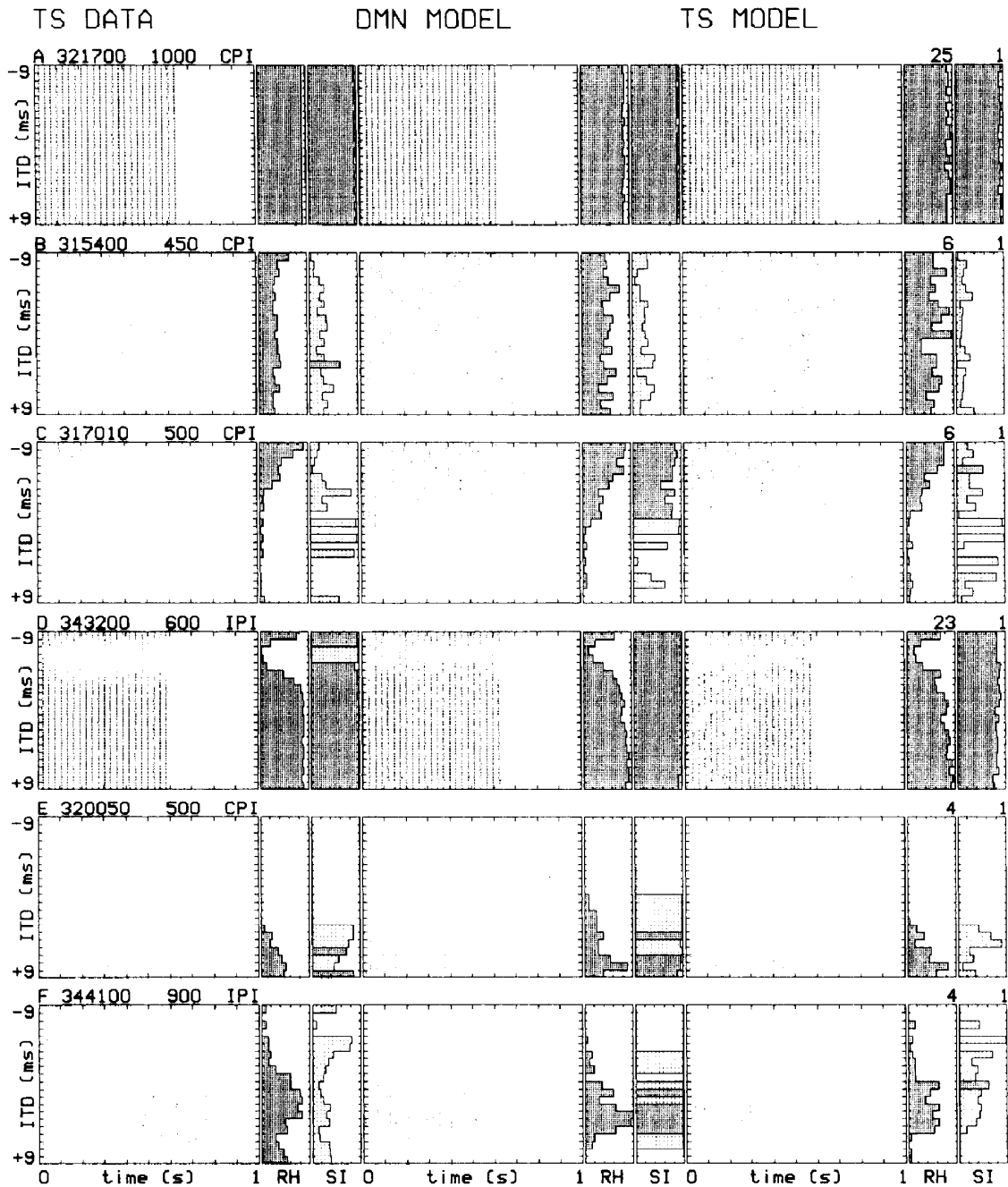


Fig. 3. Responses to ITD stimulation. A unit's sensitivity for ITD was represented by an event display reordered according to ITD. Each dot indicates the occurrence of a neural event. Horizontally, time relative to stimulus onset is denoted, the vertical axis represents ITD. At the right side of each event display, the corresponding ITD-rate histogram (RH) and ITD-SI histogram (SI) are drawn. In the SI histogram a not significant synchronization index ( $P > 0.025$ ) is indicated by a less dense grey-shading. Scaling numbers, indicated above the rate and SI histogram in the third column (TS model), apply also to rate and SI histograms in the first (TS data) and second (DMN model) column. Unit identification, carrier frequency and stimulus paradigm are indicated above the event displays in the first column. Stimulus intensity was 90 dB SPL, except in (d), in which an intensity of 70 dB SPL was applied. In case of IPI stimulation, the given intensity applies to the most intense pulse in the train. The first column represents experimental TS data, the other two columns represent the output of the DMN and TS model neuron, respectively.

was present (mean SI = 0.21). Spontaneous discharge rate was 0.7/s. Although this unit had a flat rate histogram, it clearly received input from both ears as will be demonstrated later.

At negative ITDs, thus with the ipsilateral pulse train leading, unit 317-010 (Fig. 3c) responded with only a few spikes per presentation. Response latency was approximately 90 ms. At more positive ITDs the response vanished and spontaneous activity (3.3/s) was suppressed. Upon monaural stimulation, the ipsilateral ear was excitatory, whereas the contralateral ear exerted an inhibitory influence. Because of the asymmetrical shape of the rate histogram, this response type was termed  $A_-$  with the '-' indicating that rate was at maximum in the negative ITD domain. The ITD response width was 4.8 ms, cut-off ITD -2.5 ms and time-locking was not present (SI = 0.2).

With IPI stimulation, unit 343-200 (Fig. 3d) had a strong time-locked response (SI = 0.99) starting about 20 ms after stimulus-onset. In the rate histogram a narrow trough centered around ITD = -2.5 ms is visible. This response behaviour (T-type) was also encountered in the dorsal medullary nucleus (unpublished data).

Unit 320-050 (Fig. 3e) responded only at ITD > 0.9 ms and was therefore of the  $A_+$  type. CITD was +2.5 ms. The ipsilateral ear appeared to exert an inhibitory influence. The build-up like response starts at a latency of 210 ms and responses were moderately locked to the pulses (SI = 0.69).

An example of a unit which received excitatory input from both ears is shown in Fig. 3f. This spontaneous unit (0.3/s) had a more or less symmetrical (S type) rate histogram. Energy summation, i.e. response rate is increased by an increase in contra- or ipsilateral intensity ('OR'-neuron), and binaural coincidence detection ('AND'-neuron) may be involved in this type of response. Responses were not locked to the stimulus envelope (SI = 0.3).

#### *Distribution of response properties*

The distribution of the response types is summarized in Table I. It appeared that most of the units (64.5%) had an asymmetrical ITD-rate histogram ( $A_+$ ,  $A_-$  type). Nearly one-tenth of the units had a rate histogram with a trough (T type). This response type might be resulting from the pres-

TABLE I  
DISTRIBUTION OF RESPONSE TYPES

Type	NS	$A_+$	$A_-$	T	S	Total
Number	22	62	7	10	7	108
Percentage	20	58	6.5	9	6.5	100

ence of short excitatory and inhibitory PSPs or was caused by the periodicity of the stimulus: an ITD of -9 ms is equivalent to an ITD of +19 ms. The aforementioned categories were excited by one ear and inhibited by the other ear. A minority (6.5%) had a symmetrical rate histogram, usually with a peak centered around ITD = 0 ms. This category of units was excited by both ears. The remaining 20% was not selective for ITD, although some of these units clearly received input from both ears, as was observed with monaural stimulation.

The relations between response type and, respectively, best frequency, latency, synchronization index, response width and cut-off interaural time difference are depicted in Fig. 4. The response type is indicated in the diagrams by means of symbols (scatter diagrams) and grey-coding (histograms).

The upper-left scatter diagram (Fig. 4a) shows that no relation was present between best frequency and latency. Except for the S-type, all categories had BFs which were equally distributed over the whole frequency range. All seven S-type units had BFs above 0.9 kHz, as shown in the cumulative frequency distribution histogram. This trend ( $P < 0.05$ ,  $\chi^2 = 8.06$ ,  $df = 3$ ) is in accordance with the overrepresentation of bilaterally excitable units in the high frequency domain (Epping and Eggermont, 1985b; Melssen and Epping, 1990). Similarly, the relation between spectral selectivity and selectivity for ITD was examined (not shown in figure). Most units (78%) were broadly tuned to frequency and had spectral bandwidths varying from 2 up to 4.5 octaves. No significant relation was observed between bandwidth and ITD response type. For a more elaborate study on frequency selectivity and binaural interaction in the TS the reader is referred to Melssen and Epping (1990). The nonselective units tend to have shorter latencies than units selective for ITD



( $P < 0.01$ ,  $\chi^2 = 7.0$ ,  $df = 1$ ). Again, taking into account that most of the nonselective units were only excitable by one ear, this is in agreement with earlier results (Melssen and Epping, 1990).

The scatter diagram of Fig. 4b demonstrates that synchronization index and latency are negatively correlated. Units with a high SI, thus exhibiting strong time-locking to the envelope of the pulses, had short latencies, whereas units with a small SI had longer latencies. Nonselective units exhibited a stronger time-locking than units of the remaining categories ( $P < 0.01$ ,  $\chi^2 = 8.99$ ,  $df = 1$ ). All S-type units had responses which were not locked to the stimulus envelope: SI values were always less than 0.5. However, no significant relation between SI and BF was observed.

No relation was found between response type, BF and cut-off interaural time difference (Fig. 4c). The same holds for the relations between, on the one hand, CITD and, on the other hand, respectively synchronization index and spectral bandwidth (not shown). For each response type, CITDs varied within  $-4$  and  $+4$  ms. More than 70% of the CITDs, however, fell within  $-1$  and  $+1$  ms. Nonselective units were not displayed because their CITD is not defined.

The lower-right diagram (Fig. 4d) shows that no clear relation was present between response type, synchronization index and response width. Again, nonselective units were discarded. In the low SI region almost the entire range of response width values was covered (mean RW  $5.3 \pm 2.2$

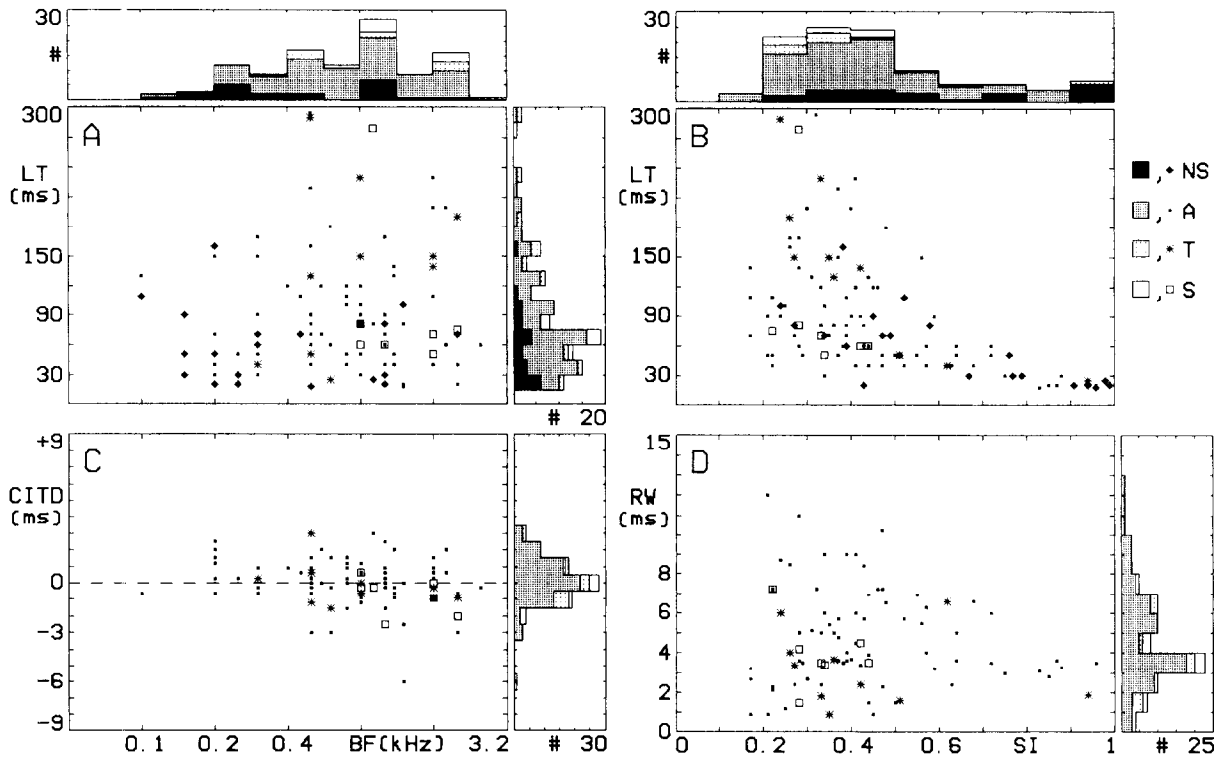


Fig. 4. Distribution of best frequency, latency, synchronization index, response width and cut-off interaural time difference. a) Scatter diagram of best frequency (BF) versus response latency (LT). Cumulative histograms of the distribution of ITD response type with respect to BF (horizontally) and LT (vertically) are represented as well. Binwidths of the histograms were 0.5 octave (BF) and 15 ms (LT), respectively. b) Scatter diagram of synchronization index (SI, horizontal axis) versus LT (vertical axis). The SI histogram (binwidth 0.1) is depicted at the top. c) Scatter diagram of BF and cut-off interaural time difference (CITD). Distribution of CITD is shown to the right. Binwidth of the histogram is 1 ms. d) Scatter diagram of SI (horizontal) versus ITD response width (RW, vertical). Binwidth of the RW histogram is 1 ms. Meaning of symbols and grey-coding is indicated at the right of the diagram in (b). NS denotes nonselectivity for ITD, A and S apply to units with an asymmetrical and symmetrical ITD-rate histogram, respectively. For T type units a trough in the rate histogram was present.

ms). It is remarkable that the lowest RW values of 1 ms were found for low SI values. For  $SI > 0.75$ , TS units had RW values varying within 2–4 ms. All except one of these units possessed asymmetrical ITD-rate histograms and had response latencies well below 30 ms (Fig. 4b).

### Stimulus invariance

In this section the invariance of ITD sensitivity to carrier frequency and absolute sound intensity level is investigated. In addition, responses obtained with CPI and IPI stimulation are compared.

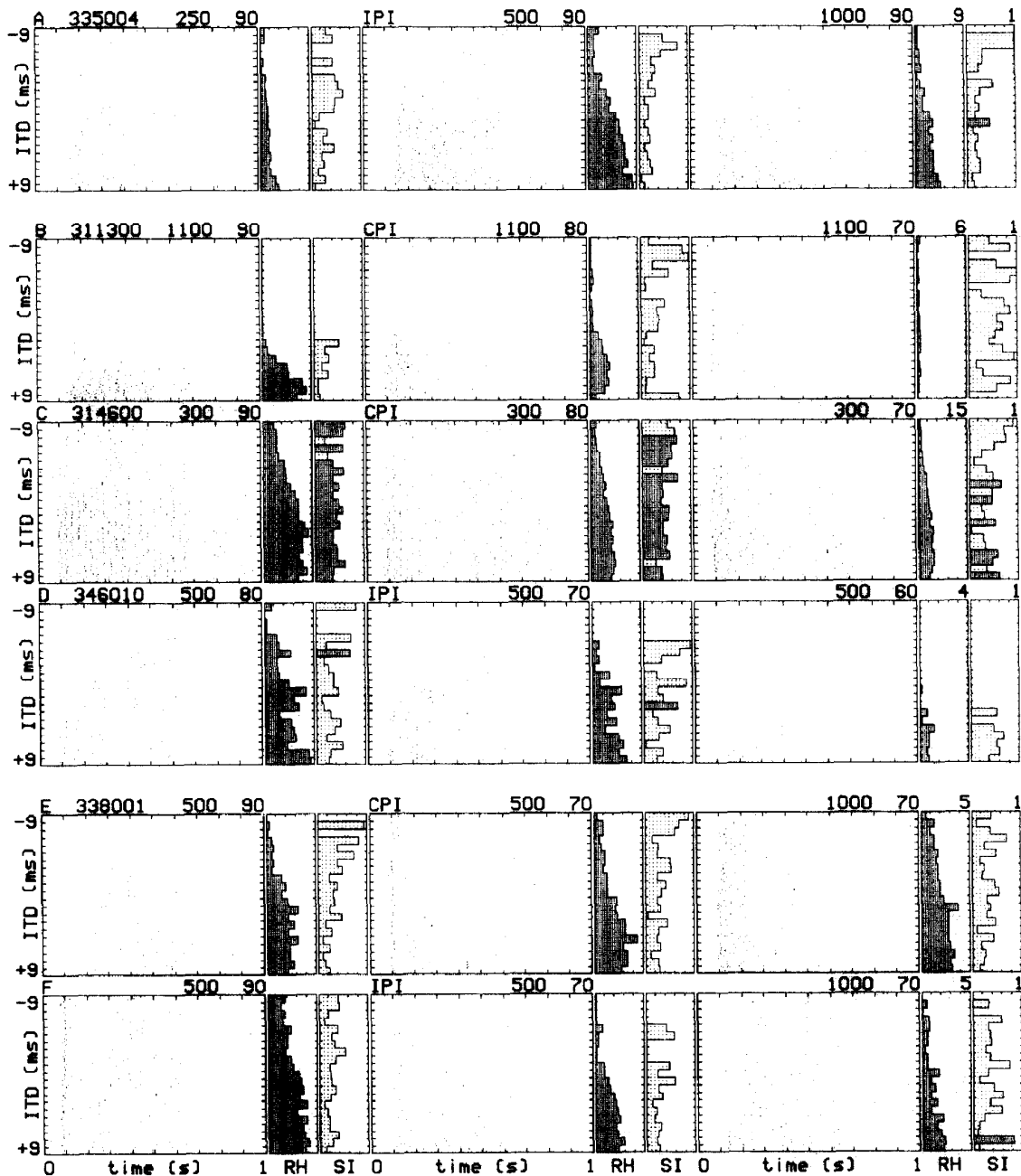


Fig. 5. Influence upon ITD selectivity of (a) carrier frequency, (b, c, d) sound intensity level and (e, f) gross stimulus envelope, i.e. CPI or IPI stimulation. Unit identification, carrier frequency and intensity are indicated above each event display. Applied stimulus paradigm is written above the event display in the second column. For more details, the reader is referred to the legend of Fig. 3.

### *Influence of carrier frequency*

The upper row in Fig. 5 represents responses of unit 335-004 to ITD stimulation (IPI paradigm, intensity 90 dB SPL) to three carriers, namely 0.25, 0.5 and 1.0 kHz. This unit with a BF of 0.5 kHz responded to the stimulus in a sustained but nonsynchronized way ( $SI < 0.4$ ). Notice the substantial latency effect at negative ITDs. Except for an overall rate effect, the temporal response patterns are very similar and ITD-rate histograms are of identical shape and differ only by a scaling factor. Response widths are 8.0, 7.5 and 6.9 ms, respectively.

In total 30 units were tested with at least two different frequencies. In general, carrier frequency was varied in steps of 1 octave with respect to BF. Twenty-one units had comparable temporal response patterns at different frequencies and rate histograms were similar, except for a scaling factor. For the remaining 9 units, the temporal response pattern or the shape of the ITD-rate histogram changed with frequency.

### *Influence of sound intensity level*

The ITD selectivity of unit 311-300 (Fig. 5b) was influenced by sound intensity. At 90 dB SPL the unit fired in a sustained way and the rate histogram was sigmoidally shaped. At a 10 dB lower level the duration of the response is shortened and the histogram becomes less peaked. At 70 dB the unit responded only to the onset of the stimulus and it was not sensitive for ITD.

The ITD selectivity of unit 314-600 (Fig. 5c) was intensity invariant. Rate histograms were identically shaped and the response width was 2.9 ms at each intensity. The number of events decreases at lower intensity levels.

At a 80 dB level (Fig. 5d), a long response latency ( $LT > 400$  ms) can be observed for negative ITDs. At lower stimulus intensities, the rate histogram shifts towards the positive ITD direction and becomes more peaked.

Twenty units were stimulated at two or more intensity levels. Of three units (15%) the ITD response type changed with intensity. Of the remaining 17 units the response type was invariant. Two of these units (10%), however, had a decreased response width at lower sound intensities,

whereas of 3 units (15%) the response width was increased substantially.

### *Influence of gross envelope: CPI versus IPI stimulation*

Seventeen units were stimulated with both CPI and IPI. Temporal response pattern, overall firing rate and response latency could vary considerably for both stimulus types. For 16 units ITD selectivity appeared to be of the same type for CPI and IPI. Of these units, 14 had comparable response widths and cut-off ITDs, whereas for 2 units significantly different RWs and CITDs were found. One unit had an asymmetrical ITD-rate histogram upon CPI stimulation and appeared to be non-selective upon IPI stimulation.

Unit 338-001 (Figs. 5e, f) was tested at two intensity levels and with two carrier frequencies. In all cases, responses were not or just weakly locked to the pulse envelope. At BF (0.5 kHz, first column), CPI stimulation evoked a sustained response pattern, whereas with IPI stimulation an onset response is present in addition. At 70 dB (second column) the response to CPI stimulation is comparable to the response as found with IPI stimulation at 90 dB. The responses at 1.0 kHz (third column) resemble closely those observed with the BF carrier at the same intensity level. In summary, the temporal response patterns for CPI and IPI stimulation differed substantially, but rate histograms were of similar shape and RWs and CITDs were approximately equal.

### *Relation between interaural time and intensity difference*

Two main ingredients in the present binaural model (See Materials and Methods) were the intensity-rate function and the intensity-latency function of NVIII fibres. In this model units will have response properties which depend on both ITD and IID and hence will exhibit a form of time-intensity trading. CPI trains were presented at BF for several ITD-IID combinations. In total, the activity of 66 neurons was recorded in 69 stimulus presentations.

Responses to combined ITD-IID stimulation of the six TS units of Fig. 3 are given in Fig. 6. In

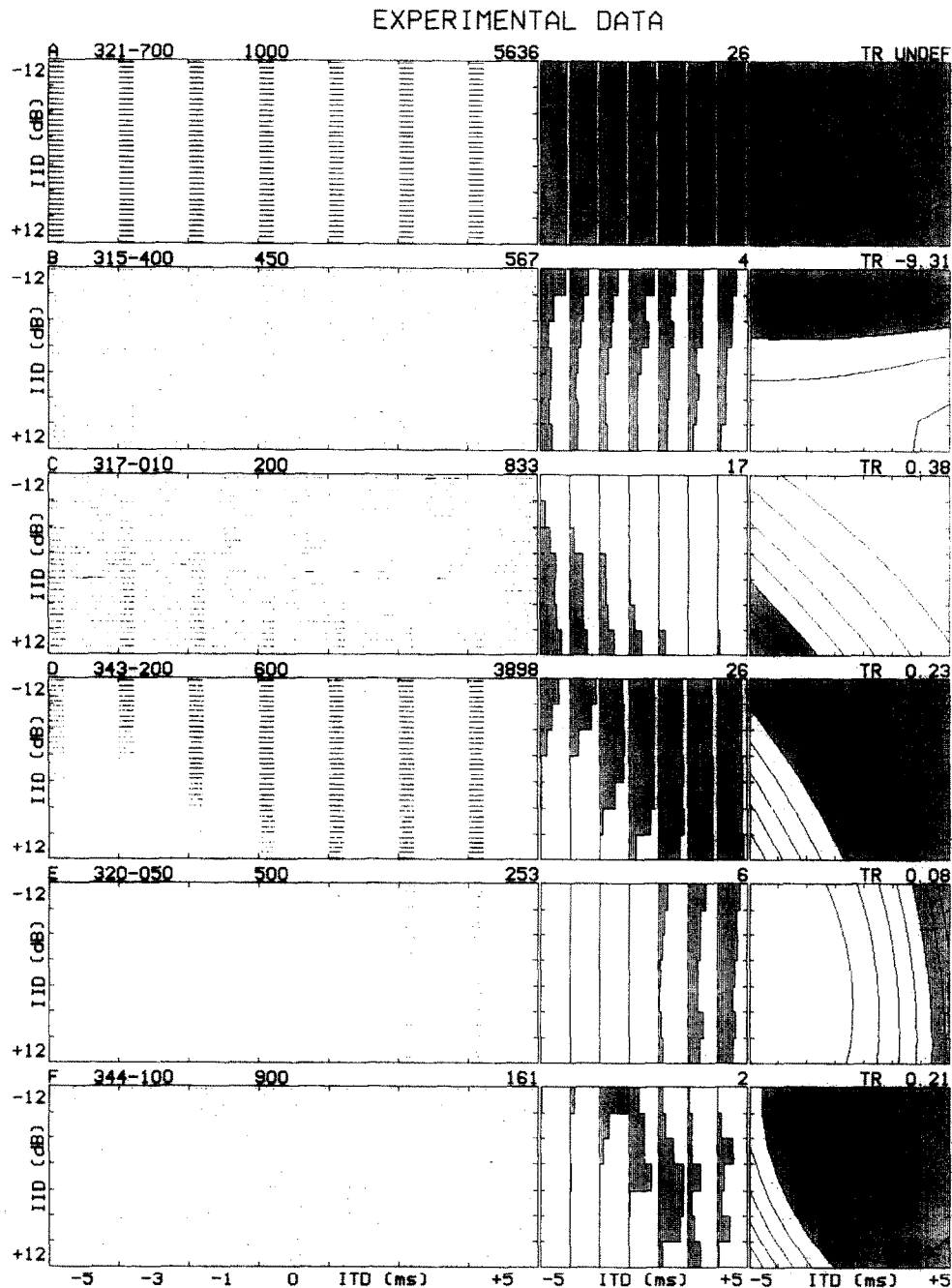


Fig. 6. Responses (experimental data) to combined ITD-IID stimulation. The event displays were reordered according to ITD (horizontal axis) and IID (vertical axis). The time between two tick-marks on the horizontal axis is three seconds, i.e. the on-set interval between two ITD-IID pulse trains. The header above each event display indicates unit identification, carrier frequency and number of recorded events. Absolute intensity level was 90 dB SPL, except in (d), in which intensity was 70 dB SPL. For each ITD, the average firing rate as function of IID was represented by vertical histograms. The left histogram corresponds to ITD = -5 ms, the right one to ITD = +5 ms. In each histogram, the vertical axis (IID) is the same as in the event display. The scaling number provided above the right histogram applies to all histograms. At the most right, the iso-rate contour diagram of the fitted two-dimensional rate function  $f(\Delta T, \Delta I)$  (Eq. 1) is drawn. Each line connects points of equal rate in the ITD-IID plane. Horizontal (ITD) and vertical (IID) axes are the same as in the event display. In the grey shaded areas firing rates were greater than 50% of the maximum rate. The value of the obtained trading ratio (TR) is written above each iso-rate contour. In case of a nonselective response (a), the TR was undefined (undef).

both situations stimuli were presented at the same contralateral intensity.

The response of the monaural unit 321–700 (Fig. 6a) was not influenced by ITD and IID, which could be expected. For such nonselective units the TR was undefined.

The firing rate of unit 315–400 (Fig. 6b) decreased gradually when IID was increased. As could be expected from Fig. 3b, the response was not influenced by ITD. The trading ratio was  $-9.31$  ms/dB. In the iso-rate plot, the IID sensitivity is indicated by almost horizontal lines. Note, that the TR value is inversely proportional with the slope of the lines in the iso-rate diagram.

A nice example, in which interaural time difference was traded by a difference in interaural intensity is given in Fig. 6c. Notice the transition from total inhibition to excitation in each ITD column. The border of the transition shifts towards positive IIDs when ITD is increased. This unit had a trading ratio of  $0.38$  ms/dB, indicating that an increase of  $1$  dB in IID could be compensated by an interaural time-shift of  $+0.38$  ms.

Also unit 343–200 (Fig. 6d) exhibited time-intensity trading. Here, the transition from excitation to total suppression is very abrupt: a particular combination of ITD and IID is encoded in a typical all or none response. Compared with Fig. 6c, the trading was confined to a smaller ITD region ( $\text{ITD} < 0$  ms). The lines in the iso-rate diagram were oriented more steeply, which also is expressed by a smaller trading ratio of  $0.23$  ms/dB.

The unit of Fig. 6e responded only for  $\text{ITD} > 1$  ms. At negative ITDs, the excitation, originating from the contralateral ear, was overruled by ipsilaterally induced inhibition. Firing rate was not influenced by IID, the trading ratio was  $0.08$  ms/dB.

Evidence for the presence of binaural coincidence detection is provided by unit 344–100 (Fig. 6f). The timing of the ipsi- and contralateral pulses appeared to be crucial for this unit. Given an optimum ITD-IID combination, an increase in IID, which causes shorter response latencies in the ipsilateral NVIII, has to be compensated with a delay of the ipsilateral stimulus to re-establish the temporal match between ipsilateral and contralateral pulses. In case of only energy summation, the unit would have responded to a wider

TABLE II

DISTRIBUTION OF TIME-INTENSITY TRADING TYPES

Type	Number	%	Parameters	Binaural type
NS	3	5	$a_0$	E0
IID	13	19	$a_0, a_2, a_5$	EI
ITD-IID	41	62	$a_0, a_1, a_2$	EI (38), EE (3)
ITD	3	5	$a_0, a_1, a_4$	EI
Complex	6	9	$a_0 - a_5$	EI (5), EE (1)
Total	66	100		

Units were nonselective (NS), exclusively selective for ITD or IID, or exhibited time-intensity trading (ITD-IID). The most significant parameters of the rate function  $f(\Delta T, \Delta I)$  are listed in the fourth column. The binaural interaction type was derived from the response type (E excitatory; I inhibitory; 0 zero effective) to contra- and ipsilateral stimulation, respectively.

range of ITDs in the positive IID plane. The trading ratio coefficient ( $0.21$  ms/dB) is comparable to the TR values of the units depicted in Figs. 6c,d.

Results are summarized in Table II. Responses were divided into 4 categories: nonselective, IID selective, combined ITD-IID selective and ITD selective. A unit was considered purely IID selective in case its trading ratio was at least  $3.0$  ms/dB, whereas pure ITD selectivity corresponded to a trading ratio less than  $0.1$  ms/dB. For about one-tenth of the units the rate-fit and corresponding TR value were unreliable, as was indicated by a large mean square error. These units fell in the additional 'complex' category. The most significant parameters of  $f(\Delta T, \Delta I)$  (Eq. 1) are listed in the fourth column of Table II. The type of binaural interaction is indicated in the last column.

For 62% of the TS units, time could be traded by intensity: mean TR was  $0.46 \pm 0.2$  ms/dB. Most of these units were excited by one ear and inhibited by the other (EI), the remaining units could be excited by each ear (EE). For nearly all EI units,  $f(\Delta T, \Delta I)$  was approximately a linear function of  $\Delta T$  and  $\Delta I$ . Apart from the parameter  $a_0$ , which is equal to the average firing rate at the combination  $\Delta T = 0$  and  $\Delta I = 0$ , the parameters  $a_1$  and  $a_2$  were 10–100 times as large as  $a_3 - a_5$ . For most EE units,  $a_3$  up to  $a_5$  could not be neglected. About 20% of the units was only sensi-

TABLE III

MODEL PARAMETERS FOR AUDITORY NERVE (NVIII) AND TORUS SEMICIRCULARIS (TS)

Parameters	Value	Equation	Related to
$I$	60 dB	2, 3, 4	stimulus
$R_0, \alpha, m$	20/s, 0.15, 10 dB	2	NVIII rate
$L_0, \beta$	1.5 ms, 60 ms·dB	3	NVIII latency
$e_0, \tau_d, \tau_u$	5, 30 ms, 5 ms	7, 8	input to TS

For explanation of the parameters the reader is referred to the text.

tive for IID. All of these were of the EI-type and significant parameters were  $a_0$ ,  $a_2$  and  $a_5$ . A few units appeared to be selective for ITD only ( $a_0$ ,  $a_1$  and  $a_4$ ), whereas the remainder was nonselective or complex. All nonselective units were monaural (E0).

#### The binaural model

The response of the binaural model (Fig. 2) to ITD and ITD-IID stimulation was evaluated. Our first goal was to reproduce the six neural responses depicted in the left column of Fig. 3. Most of the model parameters were held constant, unless stated otherwise. Parameters for NVIII and TS units are listed in Table III, DMN parameters are provided in Table IV. Thresholds of ipsi- and contralateral NVIII fibres were 40 dB. Both DMN and TS neurons had an absolute refractory period  $\tau_{abs}$  of 4 ms. In all simulations, the threshold  $b$  of TS pulse generation was set to zero.

TABLE IV

MODEL PARAMETERS FOR DORSAL MEDULLARY NUCLEUS (DMN) IN FIG. 3 AND FIG. 7

Figures	CL input			IL input		
	$w_c$	$\tau_{cd}$ (ms)	$\tau_{cu}$ (ms)	$w_i$	$\tau_{id}$ (ms)	$\tau_{iu}$ (ms)
<i>a</i>	50	2	0	0	0	0
<i>b</i>	10	20	20	-7	20	20
<i>c</i>	-10	15	6	10	5	2
<i>d</i>	20	2	1	-20	4	2
<i>e</i>	10	5	2	-20	10	5
<i>f</i>	10	2	1	10	2	1

For explanation of the parameters the reader is referred to the text.

In order to reproduce the shape of the actual ITD-rate histogram, time constants and strengths of the NVIII-DMN connectivities were adjusted in the model. Four identical DMN units, with different outputs due to stochastic event generation, projected onto one TS unit. The time constants of the low-pass filter  $e(t)$  (Eq. 8) were adjusted to improve the resemblance of some of the SI histograms. The output  $y(t)$  of one DMN unit and the output  $z(t)$  of the TS unit are represented in the second and third column of Fig. 3, respectively. The same parameter set was used for the combined ITD-IID stimulus. The response  $z(t)$  of the third order TS unit to the latter stimulus is given in Fig. 7.

For the monaural model unit (Figs. 3a, 7a), each contralateral pulse caused a strong but brief change in post synaptic potential of each DMN unit. The ipsilateral ear was disconnected. Because of the absolute refractory period combined with the brief rise-time, a DMN unit responded once to each pulse in a highly synchronized way. Of course, the response is neither influenced by ITD nor by IID.

Nonselectivity for ITD may also be the result of nonsynchronized responses in ipsi- and contralateral NVIII fibres. Nonsynchronized responses were obtained by using long time constants (Fig. 3b). Connectivities had opposite signs and spontaneous activity was incorporated as well ( $a = 0.7$ , Eq. 6). However, IIDs were still signalled by this unit (Fig. 7b), because the compound PSP and hence the firing probability decreased gradually with increasing ipsilateral intensity.

The A<sub>-</sub> response type (Fig. 3c) was modelled with rather long contralateral time constants of the connectivity between NVIII and DMN, the ipsilateral time constants were three times as short. The connectivity between the contralateral NVIII and the DMN was inhibitory. In contrast to the real data (first column), strong time-locking is present in the DMN unit at negative ITDs. After spatiotemporal integration by the TS unit the selectivity for ITD was preserved but time-locking vanished. The output of the artificial TS unit up on ITD-IID stimulation, closely resembles the real response (Figs. 6c, 7c). Notice, that the spontaneous activity, which is caused by spontaneous discharges of afferent DMN units, is suppressed

at negative ITDs. This phenomenon was also observed for the real neuron.

The presence of a trough in the rate histogram in Fig. 3d and a high synchronization index, are indicative for short time constants. Indeed, the

trough in the rate histogram was reproduced well. To preserve time-locking at the TS level, the time constants  $\tau_u$  and  $\tau_d$  of the low-pass filter were adjusted to 0 and 15 ms, respectively. The typical all or none response behaviour (Fig. 6d) was, to

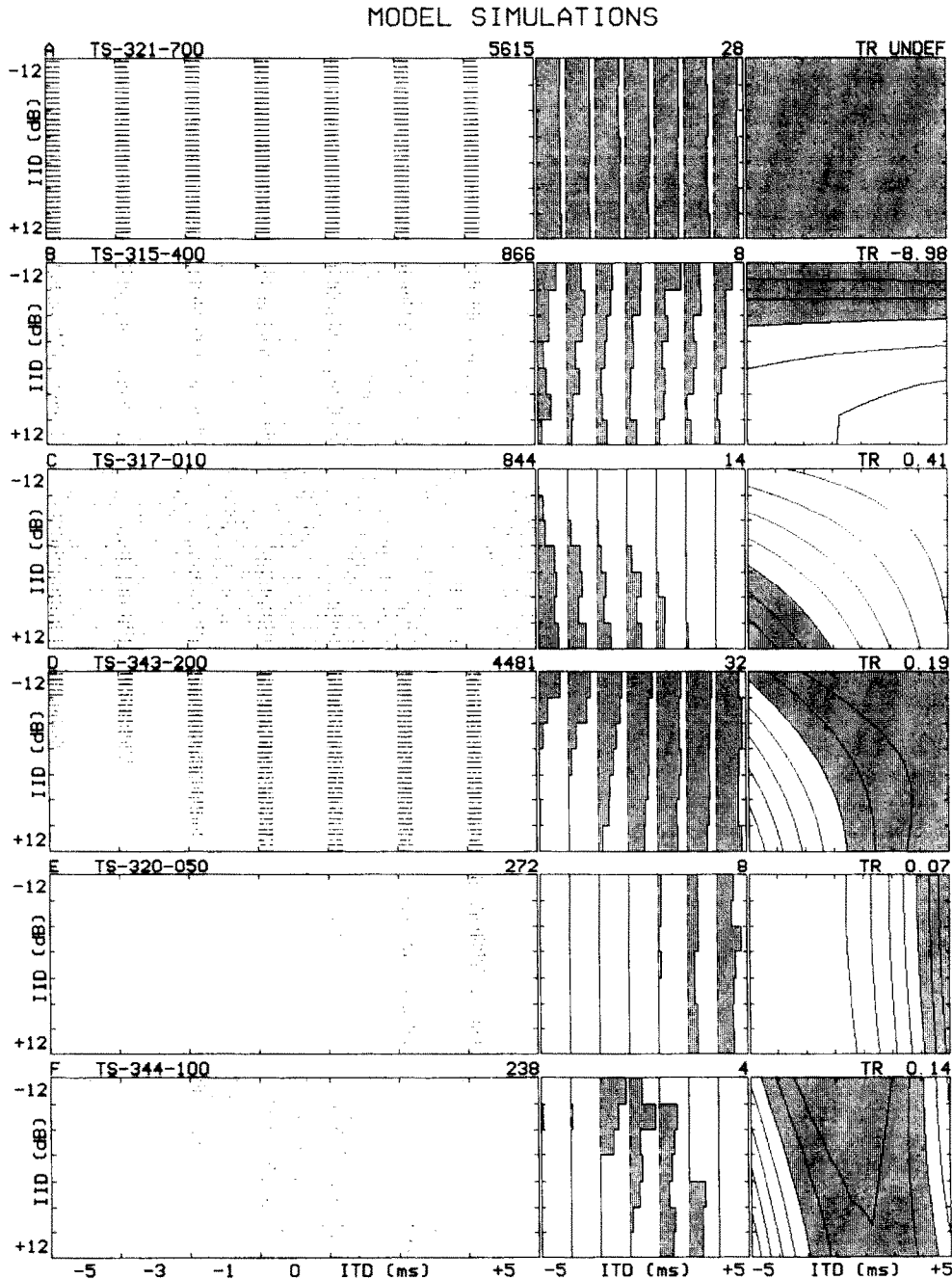


Fig. 7. Responses (simulation) to combined ITD-IID stimulation. The reader is referred to the legend of figure 6 for details. For model parameters see text and Tables III and IV.

some extent, exhibited by the model neuron (Fig. 7d) as well.

Up to here, the absolute intensity  $I$  was held at 20 dB above the threshold of both NVIII. In the simulation of Figs. 3e, 7e an intensity of 40 dB above threshold was applied. At this intensity, the NVIII rate and latency functions were saturated and hence, differences due to IID in ipsilateral and contralateral firing rate and latency were negligible. However, the timing of the excitatory and inhibitory patterns is still influenced by the externally imposed ITD. This accounts for the pure ITD sensitivity of the artificial TS unit.

We modelled the unit of Figs. 3f, 6f as a binaural coincidence detector which received excitatory input from both NVIII (cf. Kuwada and Yin, 1987). Very short time constants were applied and connectivities were excitatory. We now had to incorporate a threshold mechanism, a nonlinearity, in the pulse generation at the level of the DMN. For this purpose, the generator function  $g(u)$  was given a negative bias ( $a = -15$ ). By this mechanism, only binaural pulse-pairs with a sufficient temporal overlap will elicit time-locked DMN output. Again, spatiotemporal integration improved the form of the response pattern and the shape of the SI-histogram. The demonstrated time-intensity trading (Fig. 6f) was reproduced well by the model neuron (Fig. 7f).

In summary, by variation of time constants and strengths of the connectivities between NVIII fibres and DMN neurons the experimentally observed kinds of ITD and IID selectivity could be reproduced. Rate histograms, obtained from DMN responses, resembled closely those observed for real TS neurons. Except for the simulation of Fig. 3b, all DMN units exhibited time-locking to the stimulus pulses. The resemblance between the SI histograms, obtained by experiment and simulation, respectively, was improved (Figs. 3c, e, f) or deteriorated (Fig. 3d), due to spatial summation and temporal integration, at the level of third order TS units. However, the selectivity for ITD and IID was preserved.

## Discussion

The aim of the present study was to determine the selectivity for interaural time and intensity

difference in auditory midbrain units of the grassfrog. The proposed binaural model reproduced the observed responses upon ITD and IID stimulation successfully. In the next sections some implications on the outcome of experiments and simulations will be discussed.

### *Distribution of response types*

A large number (80%) of units in the auditory midbrain of the grassfrog appeared to be sensitive for interaural time difference. This is in accordance with the number of directional sensitive units observed with free field stimulation (Feng, 1981). Most of the binaural units had asymmetrical rate histograms ( $A_+$ ,  $A_-$ , T). For these categories a clear relation was not present between best frequency and latency (Fig. 4a), this opposed to the reciprocal BF-LT relation observed for NVIII fibres (Hillery and Narins, 1987). Presumably, spectral convergence at the level of the TS accounts for this observation. BFs varied from 0.1 up to 2.5 kHz and about 50% of the units had a BF greater than 0.8 kHz. A considerable number of units had rather long latencies ( $LT > 200$  ms), especially in the range of nonpreferred ITDs. Such long latencies might be ascribed to a near-threshold state of the neuron or disinhibition. A small number of units had a symmetrical rate histogram (S type) and could be excited by both ears. These units had BFs restricted to the high frequency range ( $BF > 0.9$  kHz), which is in accordance with earlier studies (Epping and Eggermont, 1985b; Melssen and Epping, 1990).

Using free sound field stimulation, Feng (1981) observed two different types of directional responses in the TS. Type I units, which exhibited V-shaped or inverted V-shaped directional characteristics and type II units, which possessed sigmoidally shaped directional curves. Presumably, responses of type II correspond to the  $A_+$  and  $A_-$  ITD response types, as found with dichotic stimulation, whereas the V-shaped and inverted V-shaped type I responses intuitively correspond to the T and S categories, respectively. Feng (1981) reported that no relation was present between directional response type and best frequency. Except for the high BF units with symmetrical ITD-rate histograms, present results



are in agreement with this observation. However, at least one of the two units which exhibited inverted V-shaped directional responses upon free field stimulation, also had a high BF of 1.73 kHz (Feng, 1981).

*Time-locking and selectivity for interaural time difference*

Mechanisms responsible for ITD sensitivity can be phase-locking to the sound carrier (Kuwada and Yin, 1987) and time-locking to the envelope in NVIII fibres and DMN neurons. Anuran auditory nerve fibres exhibit phase-locking up to 0.9 kHz (Hillery and Narins, 1987). The phase-locking ability of DMN neurons deteriorates rapidly above about 0.3 kHz (Van Stokkum, 1987). However, many TS neurons with  $BF > 0.3$  kHz appear to be selective for ITD. Bibikov (1977) reported considerable changes in response properties of auditory midbrain units upon variations in interaural phase difference. So, there is an apparent discrepancy between the lack of phase-locking for mid and high frequencies in DMN neurons and the phase sensitivity in the TS reported by Bibikov (1977). However, the frog's mouth was kept closed in his experiments and hence, sound could interfere in the frog's acoustic periphery. To elucidate this discrepancy, the sensitivity for interaural phase differences of some low frequency ( $BF < 0.5$  kHz) ITD-sensitive neurons was determined. For this purpose, unmodulated tonepips of 200 ms (rise- and fall-time 25 ms) were binaurally presented at BF, whereby the phase of the ipsilateral tonepip was varied between  $0^\circ$  and  $360^\circ$ . The frog's mouth was kept open. It appeared that none of the 17 units was sensitive for interaural phase differences. Hence, Bibikov's results presumably have to be ascribed to interference of soundwaves in the frog's acoustic receiver. Combining this observation with the aforementioned NVIII and DMN results, one may conclude that the role of phase-locking to the carrier in sound localization is of minor importance. Therefore, temporal locking to the sound envelope (e.g. the rise of a pulse) is the only mechanism left. This finding may have implications for binaural studies in higher vertebrates too. The use of temporally structured stimuli may elucidate ITD selectivity in high

frequency units, which often are thought to be selective for IID only.

The observed negative correlation between synchronization to the envelope and LT is very similar to the relation between phase-locking to the carrier and latency (Ribaupierre et al., 1980). In central regions of the nervous system, the degree of phase- and time-locking decreases due to an increased number of synapses in the pathway between stimulus and recorded neuron. The presence of temporal integration also may account for the loss of time-locking in the nervous system (Van Stokkum, 1990). The ITD response width of a small number of short latency TS units ( $LT < 30$  ms) with high synchronization ( $SI > 0.75$ ) was confined to the 2–4 ms range. These units had short integration times and exhibited response properties which are DMN-like. The wide range of response widths covered by long latency neurons is probably the result of spatiotemporal integration and the stochastics of event generation.

In the dorsal medullary nucleus strong time-locking to mating call pulses is observed. In the torus semicircularis only a minority of units exhibits time-locking (Eggermont and Epping, 1986; Van Stokkum, 1987). Considering that time-locking is a prerequisite for the detection of ITDs, it is advantageous to process information about binaural time and intensity disparities already in nuclei where a high degree of time-locking is still present. Indeed, in anurans the first binaural interaction takes place at the level of the DMN. About half of the units in DMN and SON receive binaural input (Feng and Capranica, 1976, 1978). Therefore, we incorporated binaural interaction already at the level of the second order units in our model.

*The relation between interaural time and intensity difference*

The appearance of a small group of neurons (5%) which were exclusively sensitive for ITD and not for IID might seem quite remarkable. In the DMN and SON, this kind of selectivity was not observed (Feng and Capranica, 1976, 1978). The latter results, however, were derived with stimulation at near-threshold intensities. In the present paper, applied intensities were about 20–30 dB

above threshold of the TS units. Afferent neurons in the DMN and SON, however, could have thresholds which were considerably lower and, moreover, might have received input from saturated NVIII fibres. In that case, the model predicts that DMN units are sensitive for ITD only (Fig. 7e).

One-fifth of the TS units are exclusively sensitive for IID. On the one hand, this might indicate that auditory midbrain units receive excitatory and inhibitory inputs. In that case, pure IID sensitivity is resulting from spatial integration and synaptic low-pass filtering (temporal integration). However, Feng and Capranica (1976, 1978) reported that a number of EI-type neurons in the DMN and SON has the same kind of sensitivity. Their observations justify the binaural interaction in the DMN in our model. Rather long time constants (Fig. 7b) were applied in the model to simulate the effect of low synchronization in the anuran auditory system.

For most auditory midbrain units (62%) ITD was traded by IID. Our data suggest that ITD and IID are not processed in separate auditory pathways, as is the case in higher vertebrates (e.g. Moiseff and Konishi, 1983). The owl, for instance, uses parallel ITD and IID pathways to localize sound in azimuth and elevation, respectively (Moiseff, 1988). In the grassfrog, ITD and IID are intricately coupled because the underlying mechanism for sound localization is to a large extent based on the comparison of differences in rate and latency between ipsilateral and contralateral NVIII fibres. Obviously, the degree of time-intensity trading is determined by the steepness of NVIII rate and latency functions (Eqs. 2, 3). Simulations showed that selectivity for ITD and IID is also highly influenced by the strength and time constants of the ipsi- and contralateral connectivities between NVIII fibres and DMN neurons (Figs. 7b–c).

#### *The role of the TS in sound localization*

At first sight one might conclude that binaural cues are processed mainly by neurons located in peripheral nuclei such as the DMN. This suggests that the role of the TS in the localization of sound is of minor importance. However, in regard to the

frequency dependent directionality of the anuran acoustic periphery (Palmer and Pinder, 1984), combined with the sharp frequency tuning of DMN and SON neurons (Feng and Capranica, 1976, 1978; Fuzessery and Feng, 1983), it is unlikely that such neurons are able to encode ITD and IID in a frequency independent way. Many neurons in the TS, on the contrary, are broadly tuned to frequency (Walkowiak, 1980; Fuzessery, 1982, 1988) and receive information about ITD and IID by means of afferent projections ascending from both ipsilateral and contralateral DMN and SON (Feng, 1986a, 1986b; Wilczynski, 1988). Moreover, units in the auditory midbrain of the grassfrog exhibit a combined sensitivity for frequency and IID, which presumably deals with the frequency dependent directionality of the acoustic periphery (Melssen and Epping, 1990). A consistent determination of sound source laterality can only be achieved by comparing interaural disparities in several frequency bands simultaneously. In view of the present data it is evident that many TS neurons possess such a property: at least 60% exhibits a selectivity for ITD which is not influenced by frequency. About the same number of units exhibited a selectivity for ITD which was invariant with respect to absolute intensity level too. Other studies reported also an abundance of units in the TS which were selective for IID in an intensity invariant way (Feng and Capranica, 1978; Melssen and Epping, 1990).

The observed intensity invariance suggests that TS units are innervated by an ensemble of DMN and SON neurons among which neural thresholds vary substantially. To illustrate this, a simulation was performed in which a TS neuron received input from eight second order units. In previous simulations, each DMN unit was innervated by ipsilateral and contralateral NVIII fibres with equal thresholds. In the present simulation a single DMN unit was innervated by NVIII fibres with the same threshold. Across DMN units, however, thresholds of incoming NVIII fibres were varied between 20 and 60 dB. Consequently, DMN thresholds will vary too and hence, an increasing number of DMN units will be recruited at higher intensity levels. As could be expected from the NVIII rate and latency functions, the degree of ITD and IID selectivity of a particular DMN unit

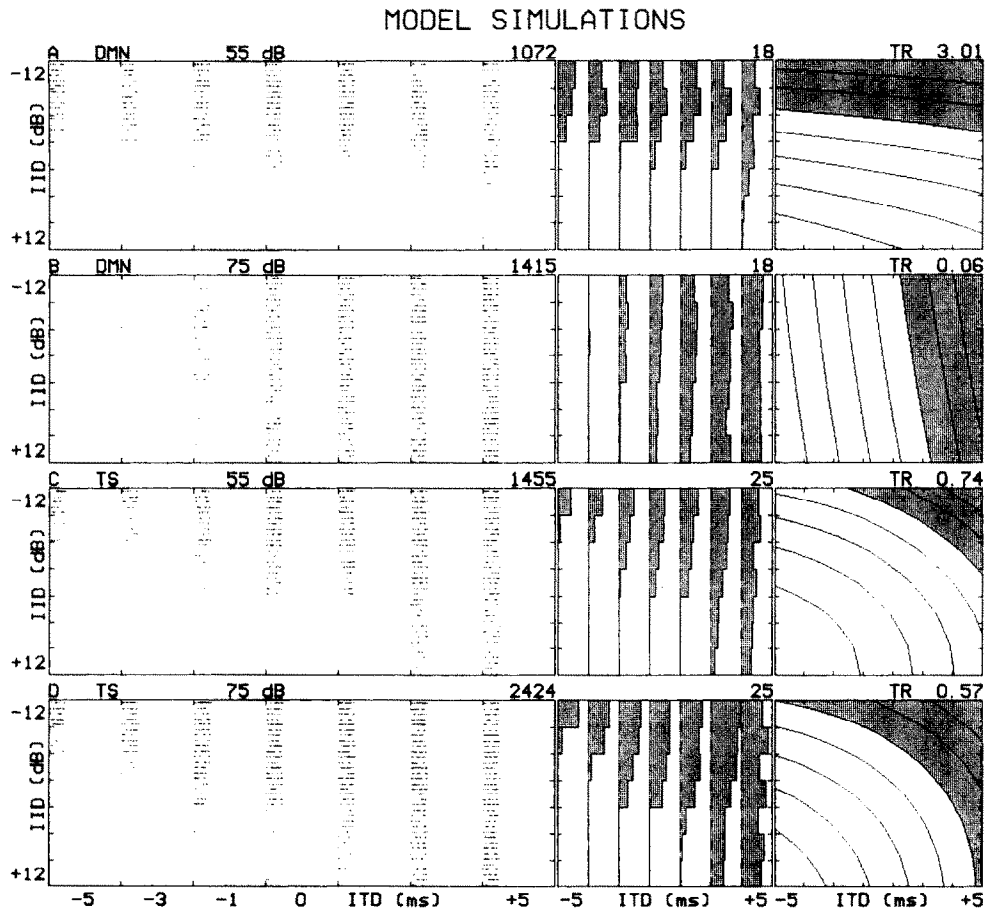


Fig. 8. Effects of overall intensity variation and spatial integration. Simulated responses of a DMN unit (a, b) and a TS unit (c, d) to ITD-IID stimulation at two intensity levels: 55 dB in (a, c) and 75 dB in (b, d). The DMN time constants were  $\tau_{cd} = 5$ ,  $\tau_{cu} = 2.5$ ,  $\tau_{td} = 15$ ,  $\tau_{tu} = 7.5$  ms. Coupling strengths were  $w_c = 10$  and  $w_e = -10$ . Each DMN unit was innervated by a group of NVIII fibres. Thresholds were identical within a group of NVIII fibres, but varied among groups: 20–60 dB. The DMN unit shown, received input from NVIII fibres each of which had a threshold of 40 dB. The TS unit received input from eight DMN neurons with different thresholds. For more details see text and legend of Fig. 6.

(NVIII thresholds 40 dB) depends strongly on the absolute intensity level (Figs. 8a, b). Except for an overall rate effect, the ITD-IID selectivity of the TS unit is hardly influenced by intensity (Figs. 8c, d). This intensity invariance results from spatio-temporal integration of activity of DMN units, which receive input from NVIII fibres with different thresholds.

With ITD-IID stimulation a mean trading ratio of +0.46 ms/dB was found, which indicates that relatively small IIDs can be resolved by TS units. This, because IID has been transformed into ITD by NVIII fibres. Moreover, the distribution of cut-off ITDs (Fig. 4c) indicates that most units are

concerned with the processing of ITDs between  $-3$  and  $+3$  ms. Considering the range of IIDs generated by the acoustic periphery, the CITDs are in the physiological range of the grassfrog (Aertsen et al, 1986). It is hypothesized that IID, and thus ITD, correspond to sound source laterality. Then, laterality of sound is encoded by an ensemble of  $A_+$  units in the TS. At negative ITDs the response of nearly all  $A_+$  units will be suppressed in the contralateral TS. Whereas at progressively larger ITDs there would be a progressive recruitment of these neurons. In such a balance model (Fay and Feng, 1987; Melssen and Epping, 1990) ITD and IID are encoded by the

relative number of recruited neurons in each torus. In higher vertebrates, because of the topographic mapping of interaural sensitivities on the neural substrate, a more elaborate *place* model has been proposed (Irvine, 1986). The CITD distribution indicates that small ITDs are represented better than large ITDs. The accuracy of sound localization may be enhanced by ensemble coding (Epping and Eggermont, 1987).

#### *Localization and identification of sound*

For a number of units, the influence of ITD was more pronounced in the later response phases (cf. Figs. 5e, f). First of all, this suggests that latencies and time constants of excitatory processes on the one hand and inhibitory processes on the other hand may differ substantially. Using monaural stimulation with random acoustic clicks, Epping and Eggermont (1986) reported that a considerable number of TS units had response patterns which were a combination of excitatory and inhibitory processes. In dichotic studies, similar excitatory and inhibitory influences, originating from the ipsi- and contralateral ear, upon the neural response pattern have been observed (Carney and Yin, 1989; Goldberg and Brown, 1969; Melssen and Epping, 1990). Secondly, the repetition of the pulses might facilitate the selectivity for ITD and IID. With monaural stimulation it was shown that units in the TS have a selectivity for pulse duration and pulse repetition rate (Van Stokkum, 1990). With binaurally presented amplitude modulated soundbursts it appeared that TS units were most selective for ITD in case amplitude modulation frequency was about 36 Hz, whereas units seldomly exhibited ITD selectivity in presence of unmodulated tones (Melssen and Van Stokkum, 1988). In the latter study it was suggested that identification and localization of sound are intricately coupled processes which make use of the same underlying neural mechanism. The present data indicate that the primary processing of binaural information has to be performed in the DMN and SON. A large number of DMN units, however, is also selective for fast intensity changes, like the onsets of the pulses in the mating call (Hall and Feng, 1988; Van Stokkum, 1987). In the TS, a more robust frequency

and intensity invariant selectivity for ITD and IID is established by spectral convergence and spatio-temporal integration. Temporal integration also enhances selectivity for pulse repetition rate (Van Stokkum, 1990). These observations indicate that, indeed, aspects of sound location and sound identity are processed simultaneously in both peripheral (DMN, SON) and central (TS) stages of the anuran auditory pathway. Therefore, it would be worthwhile to extend the present binaural model to a more complete one in which properties of the anuran auditory periphery are included. Such an extended model has to cope with a larger variety of stimulus ensembles than employed in the present study. The monaural model of Van Stokkum (1988, 1990) which deals with peripheral neural properties, together with the model of the anuran acoustic periphery (Aertsen et al., 1986) are good candidates for the extension of our binaural model.

#### *General Conclusions*

A large number of single units in the torus semicircularis exhibit a selectivity for interaural time difference which is invariant with respect to carrier frequency and sound intensity. Intensity invariant selectivity for interaural time difference can be achieved by the mechanism of spatiotemporal integration.

Most units had intricately coupled sensitivities for interaural time and intensity difference. The observed time-intensity trading patterns are mainly resulting from the intensity-rate and intensity-latency characteristics of auditory nerve fibres.

The present model, in which binaural neural interaction at the level of second order neurons was followed by spatiotemporal integration, successfully reproduced the variety of experimentally observed response patterns in the auditory mid-brain of the grassfrog.

#### **Acknowledgements**

This investigation was supported by the Netherlands Organization for Scientific Research (NWO) and by a fellowship of the Royal Netherlands Academy of Arts and Sciences (KNAW) to Willem Epping. The authors wish to thank Koos Braks for the skilful animal preparation and Thom

Oostendorp for software assistance. Stan Gielen and Peter Johannesma provided helpful comments on the manuscript.

## References

- Aertsen, A.M.H.J., Vlamming, M.S.M.G., Eggermont, J.J. and Johannesma, P.I.M. (1986) Directional hearing in the grassfrog (*Rana temporaria* L.). II. Acoustics and modelling of the auditory periphery. *Hear. Res.* 21, 17–40.
- Van Bergeijk, W.A. (1962) Variation on a theme of Békésy: a model of binaural interaction. *J. Ac. Soc. Am.* 34, 1431–1437.
- Bibikov, N. (1977) Dependence of the binaural neurons reaction in the frog torus semicircularis on the interaural phase difference. *Sechenov Physiol. J. USSR.* 63, 365–373.
- Brzoska, J., Walkowiak, W. and Schneider, H. (1977) Acoustic communication in the grassfrog (*Rana t. temporaria* L.): calls, auditory thresholds and behavioral responses. *J. Comp. Physiol.* 118, 173–186.
- Brzoska, J. (1984) The electrodermal response and other behavioral responses of the grassfrog to natural and synthetic calls. *Zool. Jb. Physiol.* 88, 179–192.
- Carney, L.H. and Yin, T.C.T. (1989) Responses of low-frequency cells in the inferior colliculus to interaural time differences of clicks: excitatory and inhibitory components. *J. Neurophysiol.* 62, 144–161.
- Cox, D.R. and Isham, V. (1980) Point processes. Chapman and Hall, London.
- Eggermont, J.J. (1985) Peripheral auditory adaptation and fatigue: A model oriented review. *Hear. Res.* 18, 57–71.
- Eggermont, J.J. and Epping, W.J.M. (1986) Sensitivity of neurons in the auditory midbrain of the grassfrog to temporal characteristics of sound. III. Stimulation with natural and synthetic mating calls. *Hear. Res.* 24, 255–268.
- Eggermont, J.J. (1988) Mechanisms of sound localization in anurans. In: B. Fritzsche et al. (Eds.), *The Evolution of the Amphibian Auditory System*, Wiley, New York, pp. 307–336.
- Epping, W.J.M. and Eggermont, J.J. (1985a) Single-unit characteristics in the auditory midbrain of the immobilized grassfrog. *Hear. Res.* 18, 223–243.
- Epping, W.J.M. and Eggermont, J.J. (1985b) Relation of binaural interaction and spectrotemporal characteristics in the auditory midbrain of the grassfrog. *Hear. Res.* 19, 15–28.
- Epping, W.J.M. and Eggermont, J.J. (1986) Sensitivity of neurons in the auditory midbrain of the grassfrog to temporal characteristics of sound. I. Stimulation with acoustic clicks. *Hear. Res.* 24, 37–54.
- Epping, W.J.M. and Eggermont, J.J. (1987) Coherent neural activity in the auditory midbrain of the grassfrog. *J. Neurophysiol.* 57, 1464–1483.
- Fay, R.R. and Feng, A.S. (1987) Mechanisms for directional hearing among nonmammalian vertebrates. In: W.A. Yost and G. Gourevitch (Eds.), *Directional hearing*. Springer Verlag, Berlin, pp. 179–213.
- Feng, A.S. and Capranica, R.R. (1976) Sound localization in anurans. I. evidence of binaural interaction in dorsal medullary nucleus of bullfrogs (*Rana catesbeiana*). *J. Neurophysiol.* 39, 871–881.
- Feng, A.S. and Capranica, R.R. (1978) Sound localization in anurans. II. Binaural interaction in superior olivary nucleus of the green treefrog (*Hyla cinerea*). *J. Neurophysiol.* 41, 43–54.
- Feng, A.S. (1981) Directional response characteristics of single neurons in the torus semicircularis of the leopard frog (*Rana pipiens*). *J. Comp. Physiol. A* 144, 419–428.
- Feng, A.S. and Shofner, W.P. (1981) Peripheral basis of sound localization in anurans. Acoustic properties of the frog's ear. *Hear. Res.* 5, 201–216.
- Feng, A.S. (1982) Quantitative analysis of intensity-rate and intensity-latency functions in peripheral auditory nerve fibers of northern leopard frogs (*Rana P. Pipiens*). *Hear. Res.* 6, 241–246.
- Feng, A.S. (1986a) Afferent and efferent innervation patterns of the superior olivary nucleus of the leopard frog. *Brain Res.* 364, 167–171.
- Feng, A.S. (1986b) Afferent and efferent innervation patterns of the cochlear nucleus (dorsal medullary nucleus) of the leopard frog. *Brain Res.* 367, 183–191.
- Fuzessery, Z.M. and Feng, A.S. (1982) Frequency selectivity in the anuran auditory midbrain: single unit responses to single and multiple tone stimulation. *J. Comp. Physiol.* 146, 471–484.
- Fuzessery, Z.M. and Feng, A.S. (1983) Frequency selectivity in the anuran medulla: excitatory and inhibitory tuning properties of single neurons in the dorsal medullary and superior olivary nuclei. *J. Comp. Physiol.* 150, 107–119.
- Fuzessery, Z.M. (1988) Frequency tuning in the anuran central auditory system. In: B. Fritzsche et al. (Eds.), *The Evolution of the Amphibian Auditory System*, Wiley, New York, pp. 253–273.
- Goldberg J.M. and Brown P.B. (1969) Response of binaural neurons of dog superior olivary complex to dichotic tonal stimuli: Some physiological mechanisms of sound localization. *J. Neurophysiol.* 32, 613–636.
- Hall, J.C. and Feng, A.S. (1988) Influence of envelope rise time on neural responses in the auditory system of anurans. *Hear. Res.* 36, 261–276.
- Hillery, C.M. and Narins, P.M. (1987) Frequency and time domain comparison of low-frequency auditory nerve fiber responses in two anuran amphibians. *Hear. Res.* 25, 233–248.
- Irvine, D.R.F. (1986) The auditory brainstem. A review of the structure and function of auditory brainstem processing mechanisms. In: H. Autrum, D. Ottoson, E.R. Perl, R.F. Schmidt, H. Shimazu and W.D. Willis (Eds.), *Progress in sensory physiology*. Springer Verlag, Berlin, Heidelberg, pp. 212–228.
- Irvine, D.R.F. (1987) A comparison of two methods for the measurement of neural sensitivity to interaural intensity differences. *Hear. Res.* 30, 169–180.
- Itoh, K. (1984) A neuro-synaptic model of bilateral interaction in auditory nervous system. *Trans. IECE Japan Vol. E* 67, No. 1, 12–18.

- Klump, G.M. and Gerhardt, H.C. (1989) Sound localization in the barking treefrog. *Naturwissenschaften* 76, 35–37.
- Kuwada, S. and Yin, T.C.T. (1987) Physiological studies of directional hearing. In: W.A. Yost and G. Gourevitch (Eds.), *Directional hearing*. Springer Verlag, Berlin, pp. 146–176.
- Lawson, C.L. and Hanson, R.J. (1974) Solving least squares problems. Prentice-Hall, Englewood Cliffs, N.J.
- Mardia, K.V. (1972) Statistics of directional data. Academic Press, London.
- Megela, A.L. and Capranica, R.R. (1981) Response patterns to tone bursts in peripheral auditory system of anurans. *J. Neurophysiol.* 46, 465–478.
- Melssen, W.J. and Epping, W.J.M. (1990) A combined sensitivity for frequency and interaural intensity difference in neurons in the auditory midbrain of the grassfrog. *Hear. Res.* 44, 35–50.
- Melssen, W.J. and Van Stokkum, I.H.M. (1988) Selectivity for interaural time-difference and amplitude modulation frequency in the auditory midbrain of the grassfrog. In: H. Duifhuis, J.W. Horst and H.P. Wit (Eds.) *Basic issues in hearing*, Academic Press, London, pp. 279–284.
- Michelsen, A., Jørgensen, M., Christensen-Dalsgaard J. and Capranica, R.R. (1986) Directional hearing of awake, unrestrained treefrogs. *Naturwissenschaften* 73, 682–683.
- Moiseff, A. and Konishi, M. (1983) Binaural characteristics of units in the owl's brainstem auditory pathway: Precursors of restricted spatial receptive fields. *J. Neurosci.* 3, 2553–2562.
- Moiseff, A. (1988) Binaural disparity cues available to the barn owl for sound localization. *J. Comp. Physiol.* 164, 629–636.
- Narins, P.M., Ehret, G. and Tautz, J. (1988) Accessory pathway for sound transfer in a neotropical frog. *Proc. Natl. Acad. Sci. USA* Vol. 85, 1508–1512.
- Palmer, A.R. and Pinder, A.C. (1984) The directionality of the frog ear described by a mechanical model. *J. Theor. Biol.* 110, 205–215.
- Pinder, A.C. and Palmer, A.R. (1983) Mechanical properties of the frog ear: Vibration measurements under free and closed-field acoustic conditions. *Proc. R. Soc. Lond. B* 219, 371–396.
- Rall, W. (1977) Core conductor theory and cable properties of neurons. In: *Handbook of Physiology*, Sect. 1: The nervous system, Vol. 1: Cellular biology of neurons, Part 1, American Physiological Society, Bethesda ML, 39–97.
- Rheinländer, J., Gerhardt, H.C., Yager, D.D. and Capranica, R.R. (1979) Accuracy of phonotaxis by the green treefrog (*Hyla Cinerea*). *J. Comp. Physiol. A* 133, 247–255.
- Ribaupierre, F. de, Rouiller, E., Toros, A. and Ribaupierre, Y. de (1980) Transmission delay of phase-locked cells in the medial geniculate body. *Hearing Res.* 3, 65–77.
- Schneider-Lowitz, B. (1983) *Neuronaler Verarbeitung einfacher und komplexer Schallsignale in der Peripherie und den unteren Stationen der Hörbahn des Grasfrosches (Rana temporaria L.)*. Thesis, Bonn, F.R.G.
- Van Stokkum, I.H.M. (1987) Sensitivity of neurons in the dorsal medullary nucleus of the grassfrog to spectral and temporal characteristics of sound. *Hear. Res.* 29, 223–235.
- Van Stokkum, I.H.M. and Gielen, C.C.A.M. (1989) A model for the peripheral auditory nervous system of the grassfrog. *Hear. Res.* 41, 71–86.
- Van Stokkum, I.H.M. (1990) Modelling the response of neurons in the grassfrog to temporally structured monaural stimuli. *Hear. Res.* 43, 231–250.
- Vlaming, M.S.M.G., Aertsen, A.M.H.J. and Epping, W.J.M. (1984) Directional hearing in the grassfrog (*Rana temporaria* L.). I. Mechanical vibrations of tympanic membrane. *Hear. Res.* 14, 191–201.
- Walkowiak, W. (1980) The coding of auditory signals in the torus semicircularis of the fire-bellied toad and grass frog: responses to simple stimuli and to conspecific calls. *J. Comp. Physiol.* 138, 131–148.
- Walkowiak, W. and Brzoska, J. (1982) Significance of spectral and temporal parameters in the auditory communication of male grassfrogs. *Behav. Ecol. Sociobiol.* 11, 247–252.
- Walkowiak, W. (1984) Neuronal correlates of the recognition of pulsed sound signals in the grassfrog. *J. Comp. Physiol. A* 155, 57–66.
- Wilczynski, W. (1988) Brainstem auditory pathways in anuran amphibians. In: B. Fritzsche et al. (Eds.), *The Evolution of the Amphibian Auditory System*, Wiley, New York, pp. 209–231.
- Yin, T.C.T., Chan, J.C.K. and Carney, L.H. (1987) Effects of interaural time delays of noise stimuli on low frequency cells in the cat's inferior colliculus. III. Evidence for cross-correlation. *J. Neurophysiol.* 58, 562–583.
- Zelick, R. and Narins, P.M. (1985) Temporary threshold shift, adaptation, and recovery characteristics of frog auditory nerve fibers. *Hear. Res.* 17, 161–176.